

# Photophysical and Photochemical Properties of Anthryl-Labeled Polyimides: Fluorescence, Electron Transfer, and Photoreaction

Wei Jin Li and Marye Anne Fox\*

Department of Chemistry and Biochemistry, The University of Texas at Austin, Austin, Texas 78712

Received: July 29, 1997<sup>⊗</sup>

The photophysical and photochemical properties of two anthryl-labeled polyimides have been studied by absorption and fluorescence spectroscopy, single-photon counting, and picosecond transient absorption measurements. The observed emission decay is triexponential, with a very short-lived component of  $\sim 50$  ps being attributed to electron-transfer quenching by the polyimide backbone, a slower component of  $\sim 2$  ns assigned to excimer quenching, and a second long-lived component of  $\sim 10$  ns assigned to isolated anthryl chromophore emission. An anthryl cation radical is produced by flash excitation of the pendent anthryl chromophores. Irradiation of thin films of the anthryl-labeled polyimides at 350 nm in air results in the disappearance of the anthryl absorption bands and produces extensively photo-cross-linked polyimide thin films. Several possible photochemical reactions that might account for the disappearance of the anthryl absorption bands and subsequent photo-cross-linking are proposed.

## Introduction

Photoactive polyimides have received considerable attention in the past several years because of their potential applications as NLO materials,<sup>1–4</sup> as photoresists,<sup>5,6</sup> or in photoimaging<sup>7,8</sup> and/or microelectronics packaging materials.<sup>9</sup> In addition to their superior properties (such as high thermal stability, good mechanical properties, and low dielectric constant), aromatic polyimides are good electron acceptors and electron transport materials.<sup>10</sup> However, a significant problem associated with practical applications of polyimides is their limited processibility: most aromatic diamine- and dianhydride-based polyimides have quite low solubilities in most common organic solvents. A number of approaches have been developed to address this problem, including the introduction of hexafluoroisopropylidene groups to increase the flexibility of the backbone and to enhance solubility.<sup>11,12</sup>

Recently, a new class of aromatic polyimides containing multiple hydroxyl groups has been reported,<sup>6</sup> giving a material that is highly soluble in a number of common organic solvents including tetrahydrofuran (THF), chloroform ( $\text{CHCl}_3$ ), *N*-methylpyrrolidone (NMP), and methyl ethyl ketone (MEK). These hydroxyl-containing polyimides are particularly interesting because they provide facile and versatile scaffolds to which a donor chromophore with well-known photophysical properties (such as anthracene) can be appended. The resulting anthryl-labeled polyimides are used as models for studying photoinduced electron transfer from a pendent anthryl chromophore (donor) to the polyimide backbone (acceptor).

The synthesis and characterization of two soluble anthryl-labeled polyimides **1b** and **2b** are described (Scheme 1). Anthryl groups were attached to the hydroxyl groups through an ether linkage by a Mitsunobu reaction.<sup>13</sup> The resulting anthryl-derivatized polyimides **1b** and **2b** are highly soluble in THF,  $\text{CHCl}_3$ , NMP, and MEK. Absorption and emission spectroscopy, together with single-photon counting and transient absorption spectroscopy, were employed to investigate the photophysical properties of these anthracene-labeled polyimides in THF solution to define the efficiency of photoinduced electron transfer in **1b** and **2b**, the photochemical behavior of these

polyimides, and the utility of the photo-cross-linking of these anthryl-labeled polyimides in the solid state. These photoactive polyimides may find application in optical recording,<sup>14</sup> microelectronic packing materials,<sup>15,16</sup> and UV-curable protecting coatings. For example, an anthracene-derivatized polymer has been used as a contrast enhancement layer to produce submicron images.<sup>15</sup>

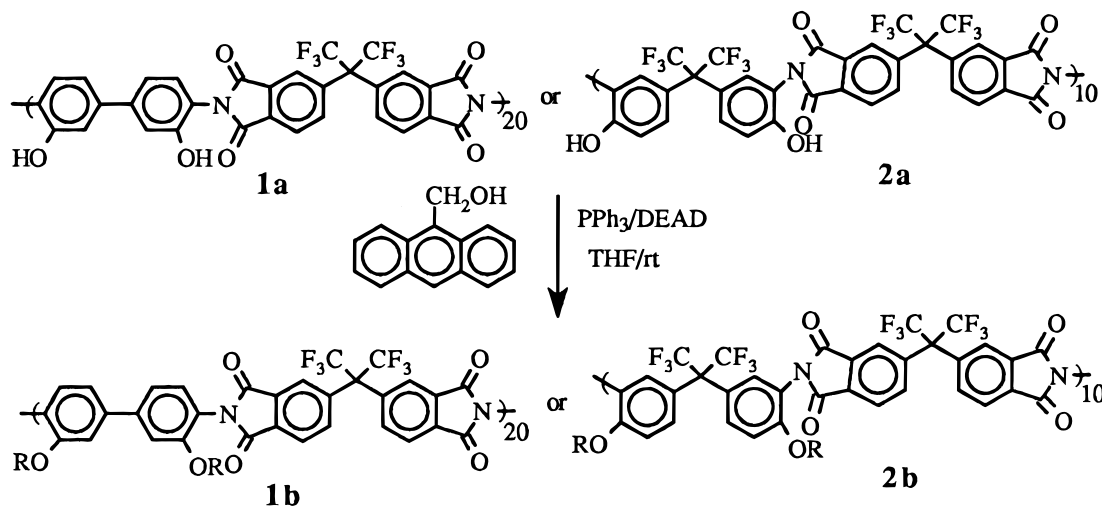
## Experiments

**Materials.** 3,3'-Dihydroxy-4,4'-diaminobiphenyl, 2,2-bis(3-amino-4-hydroxyphenyl)hexafluoropropane, and 2,2'-bis(3,4-dicarboxyphenyl)hexafluoropropane dianhydride (Chriskev) and *N,N*-dimethylacetamide (DMAc), diethyl azodicarboxylate (DEAD), and triphenylphosphine ( $\text{PPh}_3$ ) (Aldrich) were used as received. 9-Anthracenemethanol (Aldrich) was recrystallized three times from methanol before use. High-purity tetrahydrofuran (Burdick & Jackson) was used for all spectroscopic measurements. Polyimides **1a** and **2a** were prepared in high yield ( $>90\%$ ) using a procedure described by Lee et al.<sup>6</sup>

**Synthesis of Anthracene-Appended Polyimide 1b.** Polyimide **1a** (0.31 g, 0.50 mmol of repeat unit),  $\text{PPh}_3$  (0.78 g, 3.0 mmol), and 9-anthracenemethanol (0.63 g, 3.0 mmol) were dissolved in dry THF (20 mL). The flask was flushed with dry  $\text{N}_2$ , and diethyl azodicarboxylate (DEAD, 0.52 g, 3.0 mmol) was added dropwise to the solution. A red precipitate that formed immediately was dissolved into the solution after stirring at room temperature (rt) for 30 min. The reaction mixture was further stirred at rt under  $\text{N}_2$  for 48 h. After the reaction was quenched by adding several drops of acetic acid, the solution was added dropwise into a solution of methanol (300 mL) and 2 N HCl (5 mL). The collected precipitate was redissolved in THF (30 mL) and reprecipitated into a solution of methanol and HCl. The precipitate was filtered and washed with methanol to afford 0.47 g (90%) of polymer as yellow solid. Proton NMR shows a  $\geq 95\%$  loading of anthracene in **1b**:  $^1\text{H}$  NMR ( $\text{DMSO}-d_6$ )  $\delta$  6.32 (br,  $-\text{CH}_2\text{O}-$ , 4 H), 7.39–8.60 (br, aromatic protons, 30 H), 10.09 (br,  $-\text{OH}$ , residual); UV/vis (THF)  $\lambda_{\text{max}}$  ( $\epsilon \times 10^{-3}$ ,  $\text{M}^{-1} \text{cm}^{-1}$ ): 256 (71), 350, (4.7), 368 (6.2), and 387 (5.6) nm;  $\Phi_F$  (THF,  $\pm 5\%$ ): 0.06; IR (film on a KBr crystal disk): 1788, 1731, 1498, 1376, 1256, 1209, 1192, 1159  $\text{cm}^{-1}$ ; GPC:  $M_w$  ( $\times 10^4$ ) 5.1,  $M_n$  ( $\times 10^4$ ) 1.9, DSC  $T_g > 320$   $^\circ\text{C}$ , TGA 5% weight loss beginning at 405  $^\circ\text{C}$ .

<sup>⊗</sup> Abstract published in *Advance ACS Abstracts*, November 15, 1997.

## SCHEME 1: Synthesis of Anthryl-Labeled Polyimides 1b and 2b



**Synthesis of Anthracene-Labeled Polyimides 2b.** Following the same procedure as described above for preparing anthracene-labeled polyimide **1b**, 0.52 g (88%) of polymer **2b** ( $\geq 95\%$  anthracene loading) was obtained:  $^1\text{H NMR}$  (DMSO- $d_6$ )  $\delta$  6.12 (br,  $-\text{CH}_2\text{O}-$ , 4 H), 7.34–8.49 (br, aromatic protons, 30 H), 10.47 (br,  $-\text{OH}$ , residual); UV/vis (THF)  $\lambda_{\text{max}}$  ( $\epsilon \times 10^{-3}$ ,  $\text{M}^{-1}\text{cm}^{-1}$ ): 256 (71), 350 (4.4), 368 (6.2), and 387 (5.6) nm;  $\Phi_{\text{F}}$  (THF,  $\pm 5\%$ ): 0.05; IR (film on KBr crystal disk): 1788, 1731, 1498, 1376, 1256, 1209, 1192, 1159  $\text{cm}^{-1}$ ; GPC:  $M_{\text{w}}$  ( $\times 10^4$ ) 3.2,  $M_{\text{n}}$  ( $\times 10^4$ ) 1.5; DSC  $T_{\text{g}} > 290^\circ\text{C}$ , TGA 5% weight loss beginning at  $410^\circ\text{C}$ .

**Instrumentation.** Nuclear magnetic resonance (NMR) spectra were recorded on a Bruker AC-250 (250 MHz) or AC-500 (500 MHz) spectrometer. Chemical shifts are reported as  $\delta$  values relative to an internal solvent. Infrared spectra were recorded on a Nicolet 510P FT-IR spectrometer. Absorption spectra were recorded on a Shimadzu UV-3101 scanning spectrophotometer. Extinction coefficients ( $\epsilon$ ) were determined from Beer's law. Gel permeation chromatography (GPC) was conducted on four Waters Millipore  $\mu$ Styragel columns ( $10^5$ ,  $10^4$ ,  $10^3$ , and  $500 \text{ \AA}$ ) using both differential refractive index and absorption detectors. THF was used as mobile phase at a flow rate of 1.0 mL/min. Polystyrene standards (Scientific Polymer Products) were used for calibration.

Glass transition ( $T_{\text{g}}$ ) and thermal decomposition temperatures were recorded on Perkin-Elmer differential scanning calorimeter (DSC7) and thermogravimetric analyzer (TGA7), respectively, under  $\text{N}_2$ . The scanning speeds for DSC and TGA are  $40^\circ\text{C}/\text{min}$ .

Cyclic voltammetry was performed on a Princeton Applied Research 173 potentiostat. The glassy carbon electrodes were employed as working electrodes in deoxygenated acetonitrile (MeCN) containing 0.1 M tetrabutylammonium perchlorate (TBAP) as the supporting electrolyte, with a saturated calomel reference electrode (SCE) and a Pt flag (about  $0.5 \text{ cm}^2$  geometric area) as counterelectrode.

**Fluorescence Spectra.** Emission spectra in fluid solution were recorded at  $90^\circ$  on a SLM Aminco SPF-500C spectrofluorometer at room temperature. The solutions were deoxygenated by bubbling THF-saturated Ar for 20 min. The absorbances of all samples at 368 nm were adjusted to  $\sim 0.1$  (about  $2 \times 10^{-5} \text{ M}$  anthryl chromophore) to avoid aggregation and other intermolecular interactions. Fluorescence quantum

yields  $\Phi_{\text{F}}$  ( $\lambda_{\text{ex}} = 364 \text{ nm}$ ) were measured by comparing the integrated emission intensity in the region of 380–700 nm with that of an anthracene standard ( $\Phi_{\text{F}} = 0.27$ ).<sup>17</sup> Surface emission spectra ( $\lambda_{\text{ex}} = 370 \text{ nm}$ ) of anthracene-derivatized polyimide thin films on quartz plates were collected on a SPEX Fluorolog 2 instrument in the front face mode under identical conditions. The instrument contains a 450 W Xe lamp, a Hamamatsu R508 photomultiplier, and double-grating monochromators on both the excitation and emission sides of the sample compartment. The spectral data were collected on a SPEX DM3000 controller unit interfaced with the Fluorolog instrument with samples held in a special custom-designed sample holder that places the sample at a fixed distance from the excitation source and detector, allowing reproducible fluorescence intensities to be recorded.

**Fluorescence Lifetimes.** Fluorescence decays were recorded by time-correlated single-photon counting using a mode-locked, synchronously pumped, cavity-dumped pyridine I dye laser at the Center for Fast Kinetics Research at the University of Texas at Austin.<sup>18</sup> Emitted photons were collected at  $90^\circ$  with respect to the excitation beam (excited at 353 nm, monitored at 413 nm) and passed through a monochromator to a Hamamatsu Model R2809U microchannel plate. Data analysis was made after deconvolution<sup>19</sup> of the instrument response function (fwhm  $\sim 80 \text{ ps}$ ). The solutions of probe molecules in spectral grade THF were degassed by at least four freeze–pump–thaw cycles.

**Picosecond Transient Absorption.** Transient absorption spectra were carried out using  $\sim 30 \text{ ps}$  wide excitation laser pulses. Solutions of polymers in THF or polymer thin films on quartz plates were excited by the third harmonic (355 nm) pulses from a mode-locked Nd:YAG laser. The excitation intensity was attenuated with screen filters in order to prevent two-photon photoionization of the anthryl chromophores; the pulse energies were limited to  $< 10 \text{ mJ}/(\text{cm}^2 \text{ pulse})$ . The absorbance of the probe anthryl groups is adjusted between 0.3 and 0.4 for the polymer solutions and between 0.8 and 1.0 for the polymer thin films at 355 nm. Typically, 400 shots for solutions and 200 shots for thin films were averaged for each measurement.

**Thin Film Preparation and Irradiation.** Thin polymer films were spin-coated in air on quartz plates from a solution of THF–cyclohexanone (1:1) (4 wt %) using a Model P6204-A spin-coater (Specialty Coating Systems, Inc.) at a rotation speed

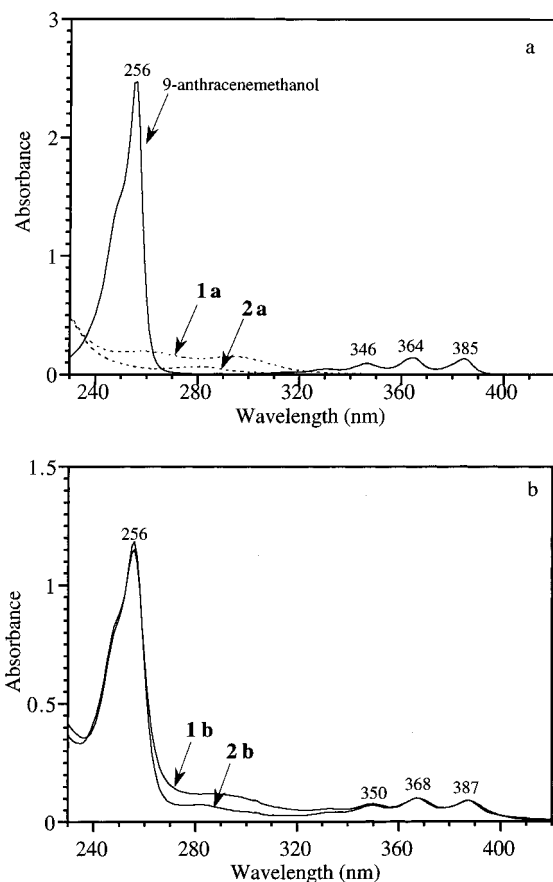


**Figure 1.** Absorption spectra of (a) polymer **1a** ( $1 \times 10^{-5}$  M of repeating unit), **2a** ( $1 \times 10^{-5}$  M of repeating unit), and 9-anthracenemethanol ( $2 \times 10^{-5}$  M) and (b) polymer **1b** and **2b** in degassed THF ( $1.5 \times 10^{-5}$  M of chromophore) at room temperature.

of 2000 rpm for 20 s. The quartz plates were cleaned by sequentially soaking in concentrated  $\text{HNO}_3$ , distilled water, and  $\text{CH}_2\text{Cl}_2$ , followed by drying under a stream of Ar. The polymer films ( $\sim 0.1 \mu\text{m}$ ) were then baked at  $100^\circ\text{C}$  for a half hour. The desired optical density of the polymer film was easily obtained by varying the solution concentration or the speed of the rotating chuck.

Irradiation of the polyimide thin films was carried out either in air or under  $\text{N}_2$ , with a Rayonet Photochemical Reactor (Southern New England Ultraviolet Co.) fitted with a set of RUL lamps blazed at  $3500 \text{ \AA}$  as monitored by absorption spectroscopy. In air, the sample plates were placed in a sample holder positioned in the photoreactor so as to ensure the same irradiation flux for all samples. Under  $\text{N}_2$ , the sample plates were placed inside a quartz photoreactor.

The polymer samples prepared for TGA studies were cast on glass slides and irradiated in air at  $350 \text{ nm}$  for 1 h. After irradiation, the polymers were scratched from the glass substrate by a razor blade and were collected as powder.

## Results and Discussion

**Photophysical Studies of Anthryl-labeled Polyimides 1b and 2b.** *A. Absorption Spectra.* Figure 1a shows the absorption bands of 9-anthracenemethanol at 256 nm ( $\epsilon = 1.3 \times 10^5 \text{ M}^{-1} \text{ cm}^{-1}$ ), 346 nm ( $\epsilon = 4.7 \times 10^3 \text{ M}^{-1} \text{ cm}^{-1}$ ), 364 nm ( $\epsilon = 7.1 \times 10^3 \text{ M}^{-1} \text{ cm}^{-1}$ ), and 385 nm ( $\epsilon = 6.6 \times 10^3 \text{ M}^{-1} \text{ cm}^{-1}$ ), whereas polyimide **1a** absorbs at 259 nm ( $\epsilon = 2.6 \times 10^3 \text{ M}^{-1} \text{ cm}^{-1}$ ) and 293 nm ( $\epsilon = 1.9 \times 10^4 \text{ M}^{-1} \text{ cm}^{-1}$ ) and polyimide **2a** at 280 nm ( $\epsilon = 1.0 \times 10^4 \text{ M}^{-1} \text{ cm}^{-1}$ ).

Anthryl chromophore loading is clearly established by the absorption spectra of **1b** and **2b** (Figure 1b), where characteristic

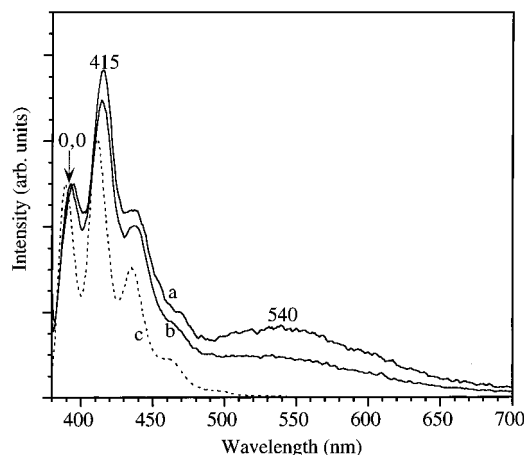


**Figure 2.** Steady-state fluorescence emission spectra ( $\lambda_{\text{ex}} = 368 \text{ nm}$ ) of (a) **2b**, (b) **1b**, and (c) 9-anthracenemethanol in deoxygenated THF ( $1 \times 10^{-5}$  M anthryl groups) at room temperature, normalized to the 0,0 band of anthracene.

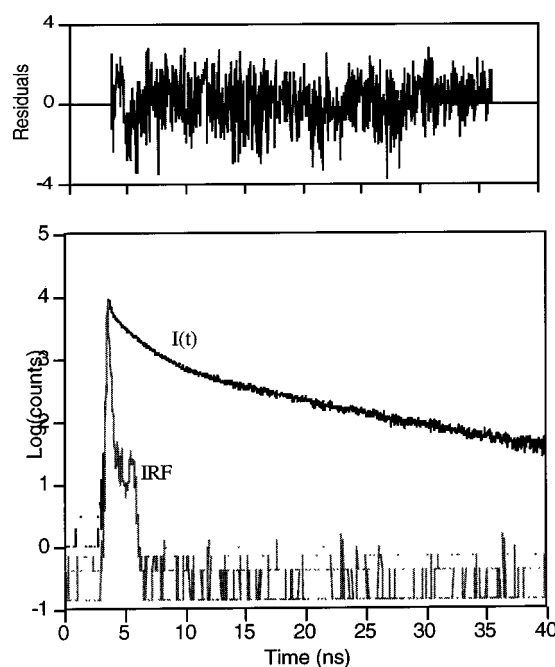


**Figure 3.** Fluorescence decay profiles  $I(t)$  of **1b** in degassed THF ( $1 \times 10^{-5}$  M) at room temperature ( $\lambda_{\text{ex}} = 353 \text{ nm}$ ,  $\lambda_{\text{em}} = 415 \text{ nm}$ ). Solid line represents a triexponential function (eq 1) superimposed on the experimental data points. Residuals showing the goodness-of-fit are depicted at the top. IRF = Instrument response function.

anthryl absorptions at 256, 350, 368, and 387 nm can be clearly seen, as well as a shoulder at around 280 nm. Because 9-anthracenemethanol does not absorb at around 280 nm where polyimides **1a** and **2a** absorb, the shoulder absorptions at around 280 nm in both **1b** and **2b** are attributed to the polyimide backbone absorption.

*B. Fluorescence Emission.* The fluorescence emission spectra (normalized to the 0,0 band of the anthryl monomer emission) of anthryl-labeled polyimides **1b**, **2b**, and 9-anthracenemethanol are shown in Figure 2. Polymers **1b** and **2b** exhibit structured monomer emission at 415 nm and weak excimer emission at around 540 nm,<sup>20</sup> whereas 9-anthracenemethanol only shows a structured monomer emission at 411 nm. On the other hand, the unlabeled polyimides **1a** and **2a** completely lack any emission in the region of 380–700 nm upon excitation at 368 nm: on the scale of Figure 3, the emission traces from **1a** and **2a** were in the baseline. Therefore,

**TABLE 1: Fluorescence Lifetimes and Transient Amplitudes Produced by Flash Excitation of Anthryl-Labeled Polyimides **1b** and **2b****

polymer	lifetime <sup>a,b</sup> (ns) (amplitude <i>A</i> )		
	$\tau_1$ ( <i>A</i> <sub>1</sub> , %)	$\tau_2$ ( <i>A</i> <sub>2</sub> , %)	$\tau_3$ ( <i>A</i> <sub>3</sub> , %)
<b>1b</b>	0.05 (85)	1.8 (11)	9.8 (4)
<b>2b</b>	0.05 (93)	1.3 (5)	8.8 (2)

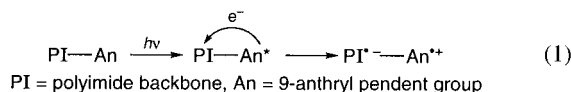
<sup>a</sup> In degassed THF at room temperature, excited at 353 nm and monitored at 415 nm. <sup>b</sup> Estimated accuracy  $\pm 10\%$ .

the emissions present in **1b** and **2b** are attributed to the appended anthryl chromophores.

The excimer/monomer emission ratio ( $I_D/I_M$ ) was estimated from the ratio of intensities of emission at its maximum (540 nm) for the excimer emission ( $I_D$ ) and at the 0,0 band (393 nm) for the isolated anthracene emission ( $I_M$ ). The  $I_D/I_M$  value of polyimide **2b** (0.34) with a more flexible chain exhibits nearly twice the excimer emission than does **1b** (0.19) with a more rigid chain. This observation suggests that anthryl chromophores in the more flexible polyimide **2b** are more easily accessible by conformational rotation for excimer formation than the more rigid polyimide **1b**, where only a fraction of anthryl chromophores are so positioned.

Excimer can be formed both between nearest neighbors and between randomly placed groups along a flexible polymer chain.<sup>20</sup> The chance for two nonnearest groups to interact to form an excimer will be much lower when appended to a rigid extended polymer backbone than a flexible one. The weak excimer emission in **1b** suggests that this polymer chain exists as a rather more rigid rod in THF at room temperature than **2b**, at least on the time scale of the excited-state lifetime. This finding is consistent with previous reports<sup>21–24</sup> that a rigid polymer backbone can suppress excimer emission by hindering the approach of the two interacting groups.

Polyimides **1b** and **2b** have very similar quantum yields for anthryl fluorescence: 0.06 and 0.05, respectively. The relatively low emission yields are likely a consequence of photoinduced electron-transfer quenching of the anthryl singlet by the polyimide backbone (eq 1) and of excimer formation. The likelihood of the proposed electron transfer was further indicated by single-photon counting measurements and was confirmed by picosecond transient absorption experiments (vide infra).



**C. Single-Photon Counting.** Time-correlated single-photon counting experiments in degassed THF at room temperature ( $\lambda_{\text{ex}} = 353$  nm,  $\lambda_{\text{em}} = 415$  nm) gave fluorescence decay profiles for the anthryl emissions in **1b** and **2b** that could be satisfactorily analyzed by a triexponential fit, with lifetimes  $\tau_1$ ,  $\tau_2$ ,  $\tau_3$  and amplitudes  $A_1$ ,  $A_2$ ,  $A_3$  ( $\sum A_i = 1.0$ ), as defined in eq 2:

$$I_f(t) = A_1 \exp(-t/\tau_1) + A_2 \exp(-t/\tau_2) + A_3 \exp(-t/\tau_3) \quad (2)$$

A typical decay trace is shown for **1b** in Figure 3. The fluorescence decay lifetimes obtained by fits to eq 2 are summarized in Table 1. Often, three-component analyses are difficult to interpret unless the likely photophysical behavior of the emissive species is known initially.<sup>25</sup> In this study, deconvolution was carried out without any assumptions about relevant decay parameters. The resulting lifetimes exhibited two components that are identical, with experimental error ( $\pm 10\%$ ), to those of similar anthracene polymers, poly(9-

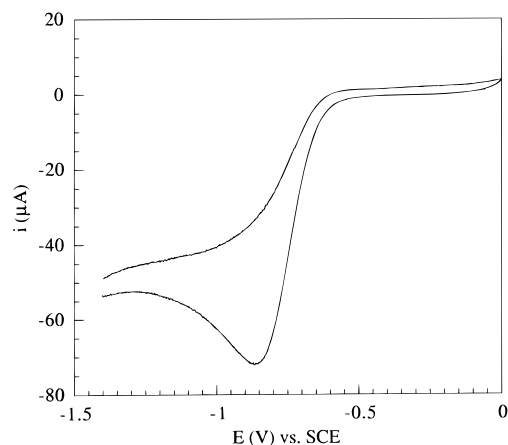


**Figure 4.** Cyclic voltammetry on a glassy carbon electrode of polyimide **1b** in deoxygenated MeCN containing 0.1 M TBAP, with a saturated calomel (SCE) as the reference and a Pt wire (about 0.5 cm<sup>2</sup> geometric area) as the counter electrode. Scan rate: 50 mV/s. Note: CV of **2b** is superimposable to that of **1b**.

anthrylmethyl methacrylate) (**9** and **2** ns) reported previously,<sup>26</sup> indicating the likely validity of the fitting analysis.

A major, very short lifetime component  $\tau_1$  ( $\sim 50$  ps) dominating the emission of anthryl-labeled polyimides, i.e., **1b** and **2b**, is attributed to electron-transfer quenching by the polyimide backbone (eq 1). Given the large amplitude ( $> 80\%$ ) of this fast component, impurity quenching is not likely. However, accurate evaluation of this short lifetime component by single-photon counting is difficult because it is close to the instrument response time of the apparatus. To prove unambiguously that photoinduced electron transfer accounted for this short-lived species, picosecond transient absorption spectroscopy was employed to detect any transient species that might be formed.

For polyimides **1b** and **2b**,  $\tau_2$  and  $\tau_3$  are virtually identical. The shorter ( $\tau_2$ ) lifetime component is assigned to anthryl groups susceptible to excimer quenching, and the longer component ( $\tau_3$ ) is assigned to isolated anthryl chromophore emission.

**D. Picosecond Transient Absorption Studies.** The rate of electron transfer is closely related to the free energy change ( $\Delta G_{\text{ET}}$ ) associated with the electron transfer. Fluorescence quenching is often nearly diffusion-controlled when  $\Delta G_{\text{ET}} \leq -10$  kcal/mol.<sup>27</sup>  $\Delta G_{\text{ET}}$  can be estimated by Rehm–Weller equation:<sup>27,28</sup>

$$\Delta G_{\text{ET}} = E_{\text{ox}} - E_{\text{red}} - \Delta E_{0-0} + C \quad (3)$$

where  $E_{\text{ox}}$  and  $E_{\text{red}}$  are the oxidation and reduction potential (in volts vs SCE) of the electron donor and acceptor, respectively,  $C$  is the Coulombic term, which is often neglected within a series of structurally similar molecules, and  $\Delta E_{0-0}$  is the spectroscopic energy of the relevant singlet or triplet excited state of donor. Here,  $E_{\text{ox}}(\text{anthracene}) = +1.3$  V (vs SCE),<sup>29</sup>  $E_{\text{red}}(\text{imide}) = -0.87$  V (vs SCE) as estimated from the cyclic voltammetric peak for **1b** (Figure 4), and  $\Delta E_{0-0}(\text{anthracene}) = 3.2$  eV (393 nm).<sup>30</sup>  $\Delta G_{\text{ET}}$  is thus estimated to be about  $-1.0$  eV (or  $-23$  kcal/mol). This suggests that photoinduced electron transfer from an excited anthryl singlet to a nearby imide moiety is thermodynamically favorable, and the rate for electron transfer ( $k_s$ ) should be very fast unless the Marcus reorganization energy is substantial.<sup>31</sup> The experimental value of  $k_s$  was estimated from time-correlated single-photon counting ( $k_s = 1/\tau_1$ ) to be  $> 10^{10} \text{ s}^{-1}$ , which is in good agreement with that predicted by eq 3.

If the proposed photoinduced electron transfer (eq 1) does occur in **1b** and **2b** upon excitation at 355 nm, one would expect

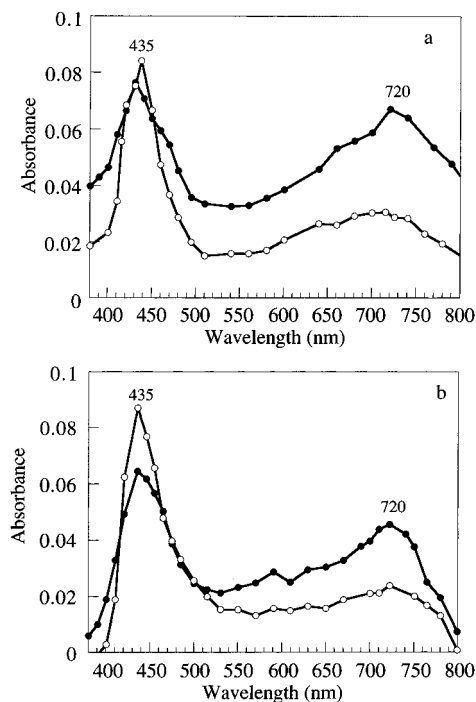


**Figure 5.** Transient absorption spectra of polyimide (a) **1b** in THF (●) and as thin film (○) and (b) **2b** in THF (●) and as thin film (○) produced by laser pulse excitation ( $\lambda_{\text{ex}} = 355$  nm,  $<10$  mJ/cm<sup>2</sup>/pulse) at delay time ( $\Delta t$ ) of 133 ps.

to detect the anthryl radical cation/polyimide radical anion pair in the transient absorption spectra. Figure 5 shows picosecond transient absorption spectra of **1b** and **2b** in degassed THF and as thin film was recorded 133 ps after laser excitation ( $\lambda_{\text{ex}} = 355$  nm) at room temperature. The transients observed are virtually identical as a dilute solution or as a film with two absorption maxima at 435 and 720 nm. The absorption spectrum of the anthracene cation radical has absorption maxima at around 435 and 720 nm, as has been previously reported by Shida<sup>32</sup> using  $\gamma$  radiolysis in *sec*-butyl chloride (*s*-BuCl), by Delaire et al.<sup>33</sup> using pulse radiolysis in cyclohexane and laser photolysis in acetonitrile, by Yamamoto et al.<sup>34</sup> using pulse radiolysis in methylene chloride, by Kira et al.<sup>35</sup> using pulse radiolysis in benzonitrile, and by Trifunac et al.<sup>36</sup> using laser flash photolysis in cyclohexane. Therefore, the absorptions at 435 and 720 nm are assigned to anthryl cation radical as a consequence of photoinduced electron transfer from a pendent anthryl singlet excited state to the polyimide backbone.

If intramolecular electron transfer is operative, the appearance of the anthryl cation radical should be accompanied by that of the polyimide anion radical. It has been reported by Freilich<sup>10</sup> that the anion radical of *N,N'*-di-*n*-pentylpyromellitic diimide (**3a**) in methylene chloride and the anion radical of Kapton polyimide (**3b**) film, generated by electron transfer from *N,N'*-

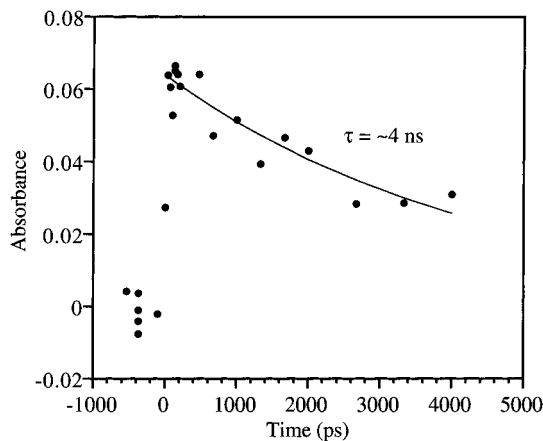
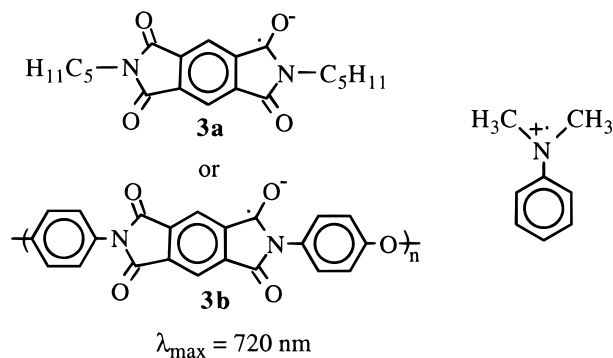


**Figure 6.** Transient absorbance measured at 720 nm for **2b** in degassed THF produced by laser pulse excitation ( $\lambda_{\text{ex}} = 355$  nm,  $<10$  mJ/cm<sup>2</sup>/pulse) at delay time. The solid line is a single-exponential fit to the experimental data points (●).

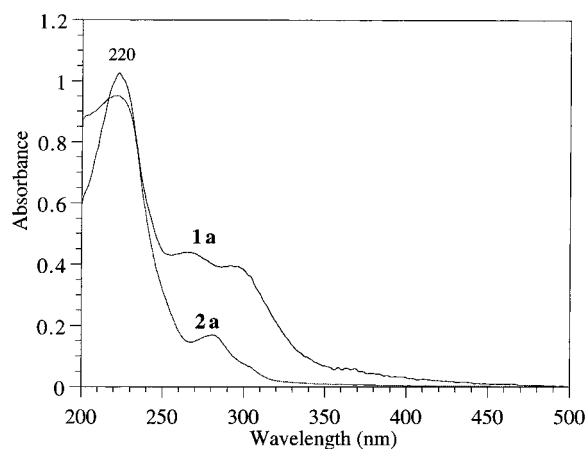


**Figure 7.** Absorption spectra of polyimides **1a** and **2a** thin films ( $\sim 0.1$   $\mu\text{m}$ ) on quartz plates.

dimethylaniline (DMA) **3a** in  $\text{CH}_2\text{Cl}_2$  or to **3b** as film upon laser flash excitation at 355 nm, both have an absorption maximum at 720 nm. Therefore, the absorption of imide anion radical would overlap with that of the anthryl cation radical at around 720 nm. The transient absorption spectra for polymer thin films of **1b** and **2b** on quartz plates are identical with those of recorded in THF solution, suggesting that the same processes operating in THF solution must also take place in the solid state.

Figure 6 shows that the decay of transient absorbance at 720 nm for **2b** in degassed THF at room temperature. The average decay lifetime was estimated to be  $\sim 4$  ns from a single-exponential fit of the experimental data. The lifetime of the appended anthryl cation radical/polyimide anion radical pair in **2b** was therefore estimated to be  $\sim 4$  ns, which is significantly shorter than that of  $\sim 50$  ns observed for the anthracene cation radical produced by laser flash photolysis of anthracene in cyclohexane saturated with  $\text{SF}_6$ .<sup>36</sup> The faster disappearance of the radical ion pair is most likely attributable to a back electron transfer from the imide anion radical to the anthryl cation radical. The average decay lifetime at 720 nm for **1b** is identical with that of **2b**,  $\sim 4$  ns.

**Irradiation of Thin Films of Polyimides 1b and 2b. A. Absorption Spectra.** The absorption spectra of thin films of polyimides **1a** and **2a** showed the absorption characteristics corresponding to those in solution (Figure 7). Both polyimides have an absorption maximum at 220 nm, whereas polyimide **1a** has two additional bands at 266 and 295 nm and polyimide **2a** has one at 280 nm. When thin films of polyimides **1a** and

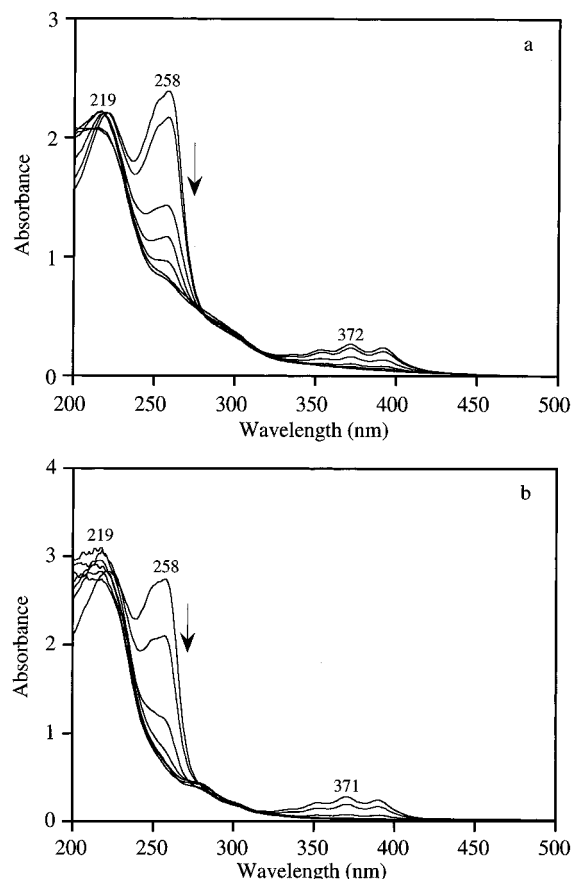


**Figure 8.** Absorption spectra of thin films ( $\sim 0.1 \mu\text{m}$ ) of (a) **1b** and (b) **2b** on quartz plates at various stage of irradiation at 350 nm. Curves in direction of arrow: 1, 3, 10, 15, 30, and 60 min of irradiation.

**2a** are subjected to irradiation at 350 nm in air for 5 h, no changes in the absorption spectra were found.

However, dramatic changes in absorption spectra of thin films of anthryl-labeled polyimides **1b** and **2b** upon irradiation at 350 nm are observed (Figure 8). In addition to the characteristic anthryl absorption bands at 258, 353, 372, and 392 nm, a band at 219 nm attributed to polyimide backbone absorptions (Figure 8) is present in both polymer absorption spectra. The long-wavelength anthryl bands (353, 372, and 392 nm) are shifted ( $\sim 4$  nm) to the red from the maximum observed in the solution phase (Figure 1), indicating the presence of significant ground-state aggregation in the thin film. Upon irradiation at 350 nm in air at room temperature, the optical densities at 258, 353, 372, and 392 nm assigned to anthryl absorptions continuously dropped. Over 95% of the anthryl absorptions had disappeared within 15 min of irradiation.

A much slower reduction in the absorbance of anthryl chromophores in polyimides **1b** and **2b** films was observed when the photolysis was conducted under  $\text{N}_2$  than in air (Figure 9). The initial drop in absorbance within 10 min of irradiation is probably due to residual  $\text{O}_2$  present in the film. An additional 2 h irradiation results in only a slight further drop in absorbance of the anthryl groups, suggesting rather inefficient photoreaction of the anthryl groups in polyimides **2b**. The same phenomenon was also observed for polyimide **1b**.

After thin films of polyimides **1b** and **2b** were irradiated in air for 1 h, they had become insoluble in an otherwise very good solvent such as THF (1 mL of THF can dissolve up to  $\sim 0.4$  g of either **1b** or **2b** at room temperature). Before irradiation, the polyimide films peeled from a quartz support after in contact with concentrated nitric acid for 5 min, but after

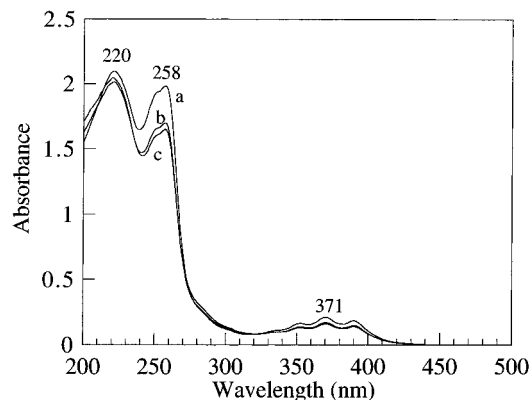


**Figure 9.** Absorption spectrum of polyimide **2b** thin film on a quartz plate (a) before and after irradiation at 350 nm under  $\text{N}_2$  for (b) 10 min and (c) 2 h.

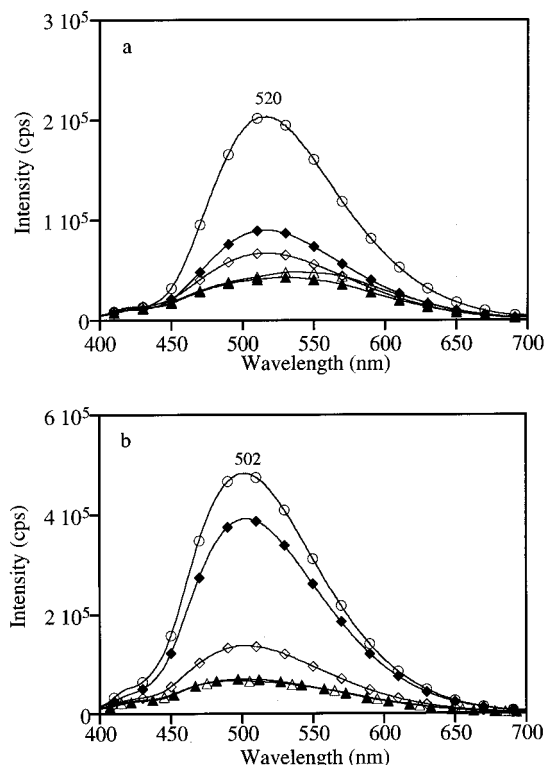


**Figure 10.** Steady-state fluorescence emission spectra for thin films of (a) **1b** and (b) **2b** after irradiation at 350 nm for 0 ( $\circ$ ), 3 ( $\blacklozenge$ ), 15 ( $\diamond$ ), 30 ( $\blacktriangle$ ), and 60 ( $\triangle$ ) min in air.

irradiation the polymer thin film stood well on the quartz support after in contact with nitric acid for 30 min.

**B. Fluorescence Emission.** Changes induced by irradiation at 350 nm in air of surface fluorescence intensity of thin films of **1b** and **2b** (Figure 10) reveal the disappearance of the broad excimer emission at 520 and 502 nm for **1b** and **2b**, respectively. Within 30 min of irradiation, the excimer emission intensities of both polymers dropped gradually, in parallel with the absorption drop at  $\sim 370$  nm. Further irradiation (beyond 30 min) results in nearly no changes in intensity in the emission spectra.

In these covalently bound rigid polyimides, diffusion of the bound anthryl chromophores is impossible. Furthermore, conformational equilibration among pendent anthryl groups is inhibited by the conformational locking imposed by the thin film matrix. Therefore, excimer emission must originate from anthryl groups already found at preformed excimer sites.<sup>37,38</sup> In a photophysical study of anthryl-labeled poly(methyl meth-

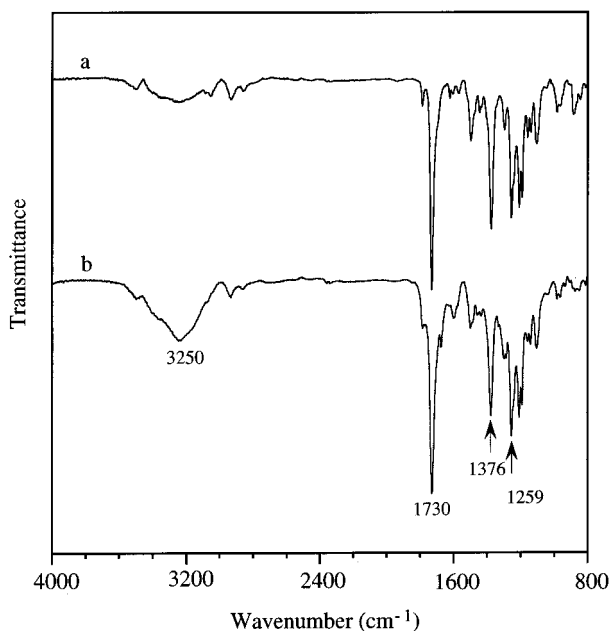


**Figure 11.** FTIR spectra of **1b** as a film on a KBr disk: (a) before irradiation and (b) after irradiation at 350 nm in air for 1 h.

acrylate) and poly(ethenyl ether), Webber and Hargreaves<sup>26</sup> have shown that excimer emission from poly(9-anthrylmethyl methacrylate) (PAMMA) and poly(9-anthryl ethenyl ether) (PAE) dominates the fluorescence spectra at room temperature when these thin film materials are formulated. They concluded that the structure giving rise to the excimer requires two anthryl groups that are partially eclipsed in PAMMA and fully eclipsed in PAE. They also attributed the larger contribution of the fully eclipsed form of anthryl excimers in PAE to higher levels of "local mobility" provided by the ether linkage of anthryl groups to PAE backbone. By analogy, two anthryl groups giving rise to the excimer emission in thin film of **1b** ( $\lambda_{\text{max}} = 520$  nm) and **2b** ( $\lambda_{\text{max}} = 500$  nm) must adopt a partially eclipsed form.

**C. Infrared Spectroscopy and TGA Studies of Polyimide 1b and 2b Upon Irradiation at 350 nm.** Infrared spectroscopy and thermal gravimetric analyses were employed to further investigate the changes in the properties of thin films of anthryl-labeled polyimides **1b** and **2b** upon irradiation at 350 nm in

air. First, a significant absorbance at  $3250\text{ cm}^{-1}$ , assigned to an  $\text{—OH}$  stretching vibration, was observed after irradiation polyimide **1b** in air (Figure 11). The incorporation of new  $\text{—OH}$  functionalities to polyimide **1b** is attributed to secondary photoproducts produced by photolysis of anthracene endoperoxide.<sup>39</sup> Second, the ratio of transmittance at  $1376\text{ cm}^{-1}$  (assigned to  $\alpha\text{—CH}_2$  deformation mode) to that at  $1730\text{ cm}^{-1}$  (assigned to  $\text{C=O}$  stretching vibration mode) are attenuated by irradiation. The reduction in the absorbance of  $\alpha\text{—CH}_2$  deformation is attributed to hydrogen atom abstraction from the methylene group adjacent to the anthryl group by free radicals produced by photolysis. The same IR changes were found in polyimide **2b** upon irradiation at 350 nm.

Before irradiation, polyimide **2b** exhibits good resistance to thermal degradation up to  $410^\circ\text{C}$  ( $<5\%$  weight loss) (Figure 12). However, after irradiation polyimide **2b** starts to lose weight at  $200^\circ\text{C}$ , suggesting that irradiation at 350 nm in air produced thermally labile functionalities such as hydroxyl groups within the polymers. The same TGA behaviors were observed for polyimide **1b** before and after irradiation at 350 nm.

Possible photoreaction pathways that might account for the observed disappearance of the anthryl groups in **1b** and **2b** and subsequent cross-linking are proposed in Scheme 2. The dominant deactivation pathway of an excited-state anthryl group, from single-photon counting and transient absorption measurements, is electron transfer (pathway 1) from the anthryl excited singlet to the polyimides **1b** or **2b** to produce the corresponding radical ion pair. In the absence of  $\text{O}_2$ , back electron transfer quenches this process. In air, the electron from the imide radical anion could be trapped by  $\text{O}_2$ , leaving an anthryl cation radical, which links to a ground-state anthracene on the same or different chain, leading to intra- or intermolecular coupling in the presence of  $\text{O}_2$ .<sup>40,41</sup> The intermolecular coupling reaction between two anthryl groups ultimately leads to cross-linking of the polyimide thin films.

Excimer is known to be a major intermediate for anthracene photodimerization in which two anthracenes are joined together through the 9- and 10-positions (pathway 2).<sup>42,43</sup> Photodimerization of anthracene or its derivatives<sup>44–49</sup> is facile in solution unless both 9- and 10-positions are blocked by two bulky groups or the required geometry for photodimerization is not attained.<sup>50</sup>

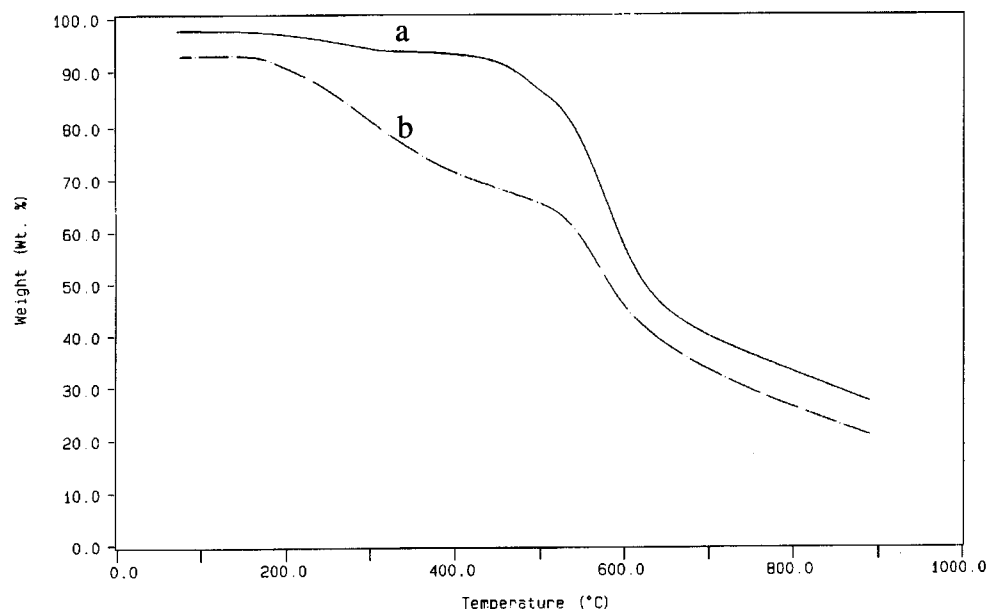
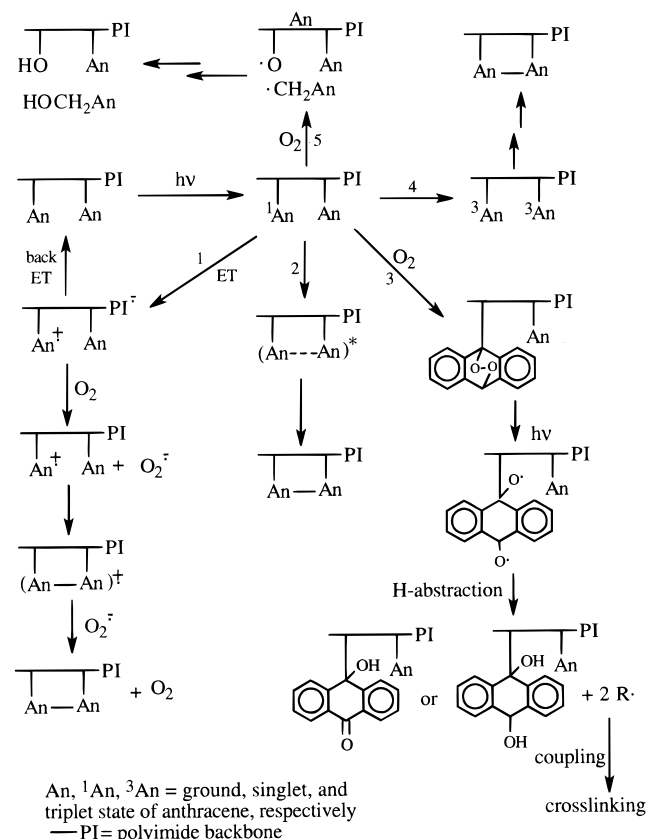


**Figure 12.** TGA curves for **2b**: (a) before irradiation and (b) after irradiation at 350 nm in air for 1 h. Heating rate of  $40^\circ\text{C}/\text{min}$  under  $\text{N}_2$ .

**SCHEME 2: Several Possible Photophysical and Photochemical Pathways Involved in Excited State of Anthryl-Labeled Polyimides 1b and 2b: (1) Electron Transfer and Anthryl Coupling, (2) Excimer Formation and Photodimerization, (3) Photooxidation, (4) Photodimerization through Triplet–Triplet Annihilation, and (5) Bond Cleavage of Aryl Ether**



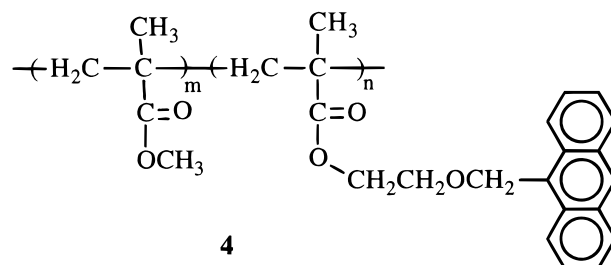
Although the anthryl groups in thin films of polyimides **1b** and **2b** exhibit excimer emission (Figure 10), attaining the required geometry for anthryl photodimerization in the rigid polyimides **1b** and **2b** thin film matrix is difficult for each pair of chromophores, as shown by rather inefficient photoreaction of the anthryl chromophores in polyimides **1b** and **2b** thin films in the absence of  $\text{O}_2$ .

On the other hand, photooxidation of anthryl chromophores in thin films of polyimides **1b** and **2b** does take place in the presence of  $\text{O}_2$  (pathway 3). Photooxidation of anthracene proceeds when an excited anthracene is quenched by a ground-state oxygen to produce singlet oxygen ( $^1\Delta_g \text{O}_2$ ) which, in turn, can react with a ground-state anthracene to generate a non-emissive 9,10-anthracene endoperoxide.<sup>15,39,49,51</sup> The endoperoxide can be easily photodegraded upon irradiation at 350 nm to produce highly reactive free radicals,<sup>52</sup> leading to the formation of secondary photoproducts<sup>53</sup> including anthraquinone, alizarin, quinizarin, and chrysazine and to subsequent cross-linking of the thin films. Dabestani and co-workers<sup>39</sup> have shown that the 9,10-anthracene endoperoxide and its secondary products account for over 80% of the photoproducts generated upon photolysis of anthracene on dry surfaces of silica and alumina (neutral) in air. By analogy, the corresponding endoperoxide generated in polyimides **1b** and **2b** thin films should be easily photodegraded upon irradiation at 350 nm to generate highly reactive free radicals that can lead to photo-cross-linking.<sup>15</sup>

Anthracene photodimerization through triplet–triplet annihilation (pathway 4) might also take place but would play a

much less important role than pathways 1 or 2 if a pendent anthryl group behaves like its freely diffusive parent.<sup>54,55</sup>

If polyimides **1b** and **2b** are to be used as resist materials, pathway 5 is of particular concern because it will retard cross-linking of the anthryl groups. Pincock and co-workers<sup>56–58</sup> have demonstrated that an aryl group can be photocleaved from its arylmethyl ester, which is likely to be responsible for the photocleavage of anthryl groups and for the main chain scission reported for poly(9-anthrylmethyl methacrylate) in degassed benzene solution<sup>26</sup> or degassed THF solution.<sup>59</sup> On the other hand, such reactivity was not observed in a solution of 2-(9-anthrylmethoxy)ethyl methacrylate and methyl methacrylate copolymer (**4**) in degassed THF solution by UV irradiation.<sup>59</sup> This latter observation suggests that the anthryl methyl ether linkage, as present in **1b** and **2b**, is photochemically stable by UV irradiation. Thus, pathway 5 can be neglected in describing the excited-state photochemistry of polyimides **1b** and **2b**, and the cross-linking consequent to pathways 1–4 can be easily observed.



## Conclusions

The anthryl-labeled polyimides **1b** and **2b** show both monomer emission at around 415 nm and weak broad, structureless excimer emission at around 540 nm in degassed THF at room temperature. The fractional contribution of excimer emission in solution correlates inversely with the rigidity of the polymer backbone; that is, the more rigid **1b** backbone suppresses excimer emission by retarding the approach of two aryl groups to the required geometry for interaction, compared with the less rigid polymer **2b**.

Single-photon counting revealed that, in addition to excimer trapping, a major, ultrafast process quenches the anthryl singlet state within ~50 ps in anthryl-labeled polyimides **1b** and **2b** in dilute THF upon laser flash excitation at 353 nm. Transient absorption spectra provide evidence for production of an anthryl cation radical and a polyimide anion radical in both THF solution and thin films. Thus, intramolecular photoinduced electron transfer from an excited anthryl chromophore (donor) to the rigid polyimide backbone constitutes a primary photo-process in these macromolecules.

Backbone rigidity plays a much less significant role in excimer formation when the polymer is examined as a thin film. In such a film, excimer fluorescence dominates the emission in both **1b** and **2b**. As a consequence, thin films of polyimides **1b** and **2b** containing pendent anthryl chromophores are easily photo-cross-linked in the solid state upon irradiation at 350 nm in air. Although several complex pathways contribute to the observed photo-cross-linking, a large change in solubility and thermal stability in the irradiated films makes **1b** and **2b** interesting as resist materials based on UV cross-linking.

**Acknowledgment.** This work was supported by the Texas Advanced Research Program and by the Robert A. Welch Foundation. We are grateful to Professor C. Grant Willson and Donald O'Connor for experimental assistance.



## References and Notes

- (1) Chen, T.-A.; Jen, A. K.-Y.; Cai, Y. *J. Am. Chem. Soc.* **1995**, *117*, 7295.
- (2) Yu, D.; Yu, L. *Macromolecules* **1994**, *27*, 6718.
- (3) Yu, D.; Gharavi, A.; Yu, L. *Macromolecules* **1995**, *28*, 784.
- (4) Verbiest, T.; Burland, D. M.; Jurich, M. C.; Lee, V. Y.; Miller, R. D.; Volksen, W. *Macromolecules* **1995**, *28*, 3005.
- (5) Chiang, W.-Y.; Mei, W.-P. *J. Polym. Sci., Polym. Chem.* **1993**, *31*, 1195.
- (6) Ho, B.; Lin, Y.; Lee, Y. *J. Appl. Polym. Sci.* **1994**, *53*, 1513.
- (7) Nakano, T. In *Proceedings of the Second International Conference on Polyimides: Synthesis, Characterization and Application*; New York, 1985; p 163.
- (8) Pfeifer, J.; Rhode, O. In *Proceedings of the Second International Conference on Polyimides: Synthesis, Characterization and Application*; New York, 1986; p 130.
- (9) Salamone, J. C., Ed. *Polymeric Materials Encyclopedia*; CRC Press: New York, 1996; Vol. 8, p 6177.
- (10) Freilich, S. C. *Macromolecules* **1987**, *20*, 973.
- (11) Mark, H. F.; Bikales, N. M.; Overberger, C. G.; Menges, G.; Kroschwitz, J. I., Eds. *Encyclopedia of Polymer Science and Engineering*; Wiley: New York, 1985; Vol. 12, p 364.
- (12) Cassidy, P. E. *Thermal Stable Polymers*; Marcel Dekker Inc.: New York, 1980.
- (13) Mitsunobu, O. *Synthesis* **1981**, 1.
- (14) Tomlinson, W. J.; Chandross, E. A.; Pork, R. L.; Pryde, C. A.; Lamola, A. A. *Appl. Opt.* **1972**, *11*, 533.
- (15) Hargreaves, J. S. *J. Polym. Sci., Polym. Chem. Ed.* **1989**, *27*, 203.
- (16) Mittal, K. L., Ed. *Polyimides: Synthesis, Characterization, and Applications*; Plenum Press: New York, 1984; Vol. 2.
- (17) Birks, J. B. *Photophysics of Aromatic Molecules*; Wiley: New York, 1970.
- (18) O'Connor, D.; Shafirovich, V. Y.; Geacintov, N. E. *J. Phys. Chem.* **1994**, *98*, 9831.
- (19) O'Connor, D. V.; Philips, D. *Time-Correlated Single Photon Counting*; Academic Press: London, 1984.
- (20) Guillet, J. *Polymer Photophysics and Photochemistry*; Cambridge University Press: New York, 1985.
- (21) Watkins, D. M.; Fox, M. A. *J. Am. Chem. Soc.* **1995**, *116*, 6441.
- (22) Watkins, D. M.; Fox, M. A. *Macromolecules* **1995**, *28*, 4939.
- (23) Fox, H. H.; Fox, M. A. *Macromolecules* **1995**, *28*, 4570.
- (24) Fox, M. A. *Acc. Chem. Res.* **1992**, *25*, 569.
- (25) Birch, D. J. S.; Imhof, R. E. *Anal. Instrum.* **1985**, *14*, 293.
- (26) Hargreaves, J.; Webber, S. E. *Macromolecules* **1984**, *17*, 235.
- (27) Weller, A. *Pure Appl. Chem.* **1982**, *54*, 1885.
- (28) Rehm, D.; Weller, A. *Isr. J. Chem.* **1970**, *8*, 259.
- (29) Bard, A. J.; Faulkner, L. R. *Electrochemical Methods: Fundamentals and Applications*; Wiley: New York, 1980.
- (30) Klessinger, M.; Michl, J. *Excited States and Photochemistry of Organic Molecules*; VCH: New York, 1995.
- (31) Marcus, R. A. *Annu. Rev. Phys. Chem.* **1964**, *15*, 155.
- (32) Shida, T. *Electronic Absorption Spectra of Radical Ions*; Elsevier: New York, 1988; p 70.
- (33) Delaire, J. A.; Castalla, M.; Fature, J. *Nouv. J. Chim.* **1984**, *8*, 231.
- (34) Yamamoto, Y.; Ma, X.-H.; Hayashi, K. *J. Phys. Chem.* **1987**, *91*, 5343.
- (35) Kira, A.; Arai, S.; Imamura, M. *J. Phys. Chem.* **1972**, *76*, 1119.
- (36) Liu, A.; Sauer, M. C.; Loffredo, D. M.; Trifunac, A. D. *J. Photochem. Photobiol. A: Chem.* **1992**, *67*, 197.
- (37) Frank, C. W.; Harrah, L. A. *J. Phys. Chem.* **1974**, *61*, 2015.
- (38) Fox, M. A.; Britt, P. F. *Macromolecules* **1990**, *23*, 4533.
- (39) Dabestani, R.; Ellis, K. J.; Sigman, M. E. *J. Photochem. Photobiol. A: Chem.* **1995**, *86*, 231.
- (40) Bard, A. J.; Ledwith, A.; Shine, H. J. In *Advances in Physical Organic Chemistry*; Gold, V., Bethell, D., Eds.; Academic Press: New York, 1976; Vol. 13, p 155.
- (41) Howarth, O. W.; Fraenkel, G. K. *J. Am. Chem. Soc.* **1970**, *92*, 6258.
- (42) Stevens, B. *Adv. Photochem.* **1971**, *8*, 171.
- (43) Saltiel, J.; Townsend, D. E.; Watson, B. D.; Shannon, P.; Finson, S. L. *J. Am. Chem. Soc.* **1977**, *99*, 884.
- (44) Bowen, E. J.; Tanner, D. W. *Trans. Faraday Soc.* **1955**, *51*, 475.
- (45) Chapman, O. L.; Lee, K. J. *Org. Chem.* **1969**, *34*, 4166.
- (46) Greene, F. D.; Misrock, S. L.; Wolfe, J. R. *J. Am. Chem. Soc.* **1955**, *77*, 3852.
- (47) Tazuke, S.; Banba, F. *J. Polym. Sci., Polym. Chem. Ed.* **1976**, *14*, 2463.
- (48) Tazuke, S.; Hayashi, N. *J. Polym. Sci., Polym. Chem. Ed.* **1978**, *16*, 2729.
- (49) Rabek, J. F. *Mechanisms of Photophysical Processes and Photochemical Reactions in Polymers: Theory and Applications*; Wiley: New York, 1987.
- (50) Cohen, M. D.; Schmidt, G. M. J. *J. Chem. Soc.* **1964**, 1996.
- (51) Zingg, S. P.; Sigman, M. E. *Photochem. Photobiol.* **1993**, *57*, 453.
- (52) Rigaudy, J.; Defoin, A.; Barnne-Lafont, J. *Angew. Chem., Int. Ed. Engl.* **1979**, *18*, 413.
- (53) Voyatzakis, E.; Vasilikiotis, G.; Alexaki-Tzivanidou, H. *Anal. Lett.* **1972**, *5*, 445.
- (54) Saltiel, J.; Marchand, G. R.; Smothers, W. K.; Stout, S. A.; Charlton, J. L. *J. Am. Chem. Soc.* **1981**, *103*, 7159.
- (55) Charlton, J. L.; Dabestani, R.; Saltiel, J. *J. Am. Chem. Soc.* **1983**, *105*, 3473.
- (56) DeCosta, D. P.; Pincock, J. A. *J. Am. Chem. Soc.* **1989**, *111*, 8948.
- (57) DeCosta, D. P.; Pincock, J. A. *J. Am. Chem. Soc.* **1993**, *115*, 2180.
- (58) Hilborn, J. W.; Pincock, J. A. *J. Am. Chem. Soc.* **1991**, *113*, 2683.
- (59) Ide, N.; Tsujii, Y.; Fukuda, T.; Miyamoto, T. *Macromolecules* **1996**, *29*, 3851.